IEEE Access
Multidisciplinary | Rapid Review | Open Access Journal

Received April 19, 2020, accepted May 26, 2020, date of publication June 9, 2020, date of current version October 8, 2020.

Digital Object Identifier 10.1109/ACCESS.2020.3001197

Comparison of AC Flashover Performance of Snow-Accreted Insulators Under Natural and Artificial Simulation Environments

YUYAO HU[1], XINGLIANG JIANG[2], (Senior Member, IEEE), SIHUA GUO[3], AND ZHONGYI YANG[2]

[1]College of Electrical and Electronic Engineering, Shandong University of Technology, Zibo 255000, China
[2]State Key Laboratory of Power Transmission Equipment and System Security and New Technology, Chongqing University, Chongqing 400044, China
[3]State Grid Chongqing Electric Power Research Institute, Chongqing 401123, China

Corresponding author: Yuyao Hu (hyuyao@sdut.edu.cn)

This work was supported by the National Natural Science Foundation of China under Grant 51907109.

ABSTRACT The research on snow-accreted insulators have been performed in an artificial climate chamber. However, the differences in the distribution, density and compactness of snow accretion under natural and artificial simulation environments cause differences in the flashover performance of snow-covered insulators. In the present work, a series of flashover tests were conducted on snow-coated glass and silicone rubber insulators in the climate chamber and at Xuefeng Mountain Natural Icing Test Base. The discrepancies in the electrical characteristics and flashover process of snow-covered insulators under two test environments were compared and analyzed. Results show that the arc flashover gradient of snow accreted insulator at high altitude site is higher than that in the laboratory because of the differences of the environmental parameters. Affected by the adiabatic effect and capillary action of snow layer, within the range of the study the flashover gradient of insulators covered with snow increases with the increasing in the snow thickness. The calculation of various forces applied on arcs during its propagation demonstrates that when the arc current is less than 0.2 A, the local arcs develop along the snow surface of the insulators under the action of an electrostatic force. As the current increases beyond 0.2 A, the thermal buoyancy is predominant, thereby causing arcs to levitate from the insulator surface.

INDEX TERMS Snow-covered insulator, flashover gradient, arc propagation, electrostatic force, thermal buoyancy.

I. INTRODUCTION

Insulator is an important facility of transmission lines, so its electrical performance plays a decisive role in the satisfactory reliability of power systems. However, ice and snow accretion on outdoor insulators considerably degrades their electric strength in cold climate regions, which leads to numerous flashover accidents in China and abroad [1]–[4]. That prompts scholars to give a great concern about iced and snow-covered insulators.

A systematic investigation on iced and polluted insulators have been carried out and achieved significant advances in the formation mechanism of ice and pollutant accumulation [5]–[7], electrical properties [8]–[10] and discharge development [11], [12]. However, less attention has been paid to the effect of snow accretion on the external insulation of transmission lines. Hu *et al*. [13] researched the effect of snow accretion on the various type of the insulators in an artificial climate chamber, and arrived at the conclusion that the relationship between the snow flashover gradient of the insulators and equivalent salt deposit density is a power function with a negative exponent. Jiang *et al*. [14] found that the DC (direct current) flashover voltage of artificial snow-covered insulator is lower than that of the AC (alternating current). Moreover, for the insulators covered with an uneven snowpack distribution, the discharge developed along the leeward side [15]. The investigation on snow disasters showed that compared with cap and pin insulator, the long rod insulator is more likely to be bridged by snowpack, thereby resulting in leakage current increasing [16]. Zhang *et al*. [17] pointed out that the water melted from snow wets the pollution on post insulator surface to form a highly conductivity water film, which is a key factor

The associate editor coordinating the review of this manuscript and approving it for publication was Xue Zhou.

FIGURE 1. Multi-functional artificial climate chamber in the laboratory.

for declining the flashover voltage. Li *et al*. [18] conducted a comparative study on the flashover characteristics of the insulators during snow accumulation and melting periods and summarized the variation rules of the flashover voltage and leakage current in different stages. Homma *et al*. [19] analyzed the influence of the electric field on the accumulating of snowpack and flashover performances of porcelain insulator and concluded that the discharges occur frequently with the increasing in water conductivity, causing snow accretion on the insulators slowing down, thereby improving its flashover voltage. Hemmatjou *et al*. [20] observed that the arc during the flashover of snow-accreted insulators is composed of the arc in airgap and the arc inside snow, which is consistent with that in the flashover process of iced insulators [21].

The preceding studies are important for the prevention and mitigation of ice and snow disaster in power systems. However, the achievements are obtained in the artificial climate chamber. The environmental parameters in the laboratory are significantly different from those in the field, which leads to the inequivalence of snow accretion on insulators and subsequent flashover characteristics between the two. Therefore, the differences in the formation mechanism and flashover characteristics of snow-accreted insulators between natural and artificial simulation environments remains poorly understood.

For these reasons, the flashover tests of snow-covered glass and silicon rubber (SIR) insulators were performed in the chamber and on site, respectively. The influences of equivalent salt deposit density (ESDD) and snow thickness (d) on the electrical performances of snow-accreted insulators were compared. From the perspective of thermodynamics, the variation of electrostatic force, electromagnetic force and thermal buoyance applied to the partial arcs during the discharge development of snow-coated insulators was calculated and analyzed, from which the phenomenon of arc floating at high altitude was explained. The purpose is to provide a reference for the external insulation design of transmission lines in snowy regions.

FIGURE 2. Xuefeng mountain natural icing test base.

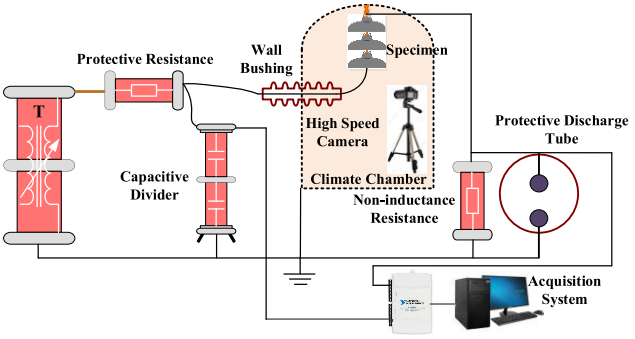

FIGURE 3. Schematic diagram of flashover tests of snow-accreted insulators.

II. TEST EQUIPMENT, SAMPLES AND PROCEDURES

A. TEST EQUIPMENT

The artificial simulation tests were performed in a climate chamber with a diameter of 7.8 m and a height of 11.8 m (Figure 1). The temperature in the chamber can be as low as –45 °C by adjusting the refrigeration system. The IEC standard nozzles are installed to generate the supercooled water droplets with the diameter of 10–120 μm. The wind speed is adjustable in the range from 0 to12 m/s.

The field examinations were carried out at Xuefeng Mountain Natural Icing Test Base (Figure 2) with typical microtopography and micrometeorological characteristics, which is the elevation of 1400 m. Icing lasts from October to March of the following year, and the annual precipitation exceeds 1800 mm. The icing duration is up to 50 days, the annual icing frequency is more than 15 times. Therefore, the test base is an ideal place to study ice and snow accretion on transmission lines.

Except that there is no climate chamber and wall bushing for the field test, the schematic diagram of flashover tests of snow-covered insulators under natural and artificial simulation environments is the same, as shown in Figure 3. The power in the chamber is supplied by an AC corona free test transformer with a rated voltage of 500 kV and a rated current of 4 A. The power is the AC source for pollution test in the field. Its rated voltage and current are 300 kV and 2 A, respectively. The rated input voltage is 10 kV and the short-circuit impedance is 7.6%.

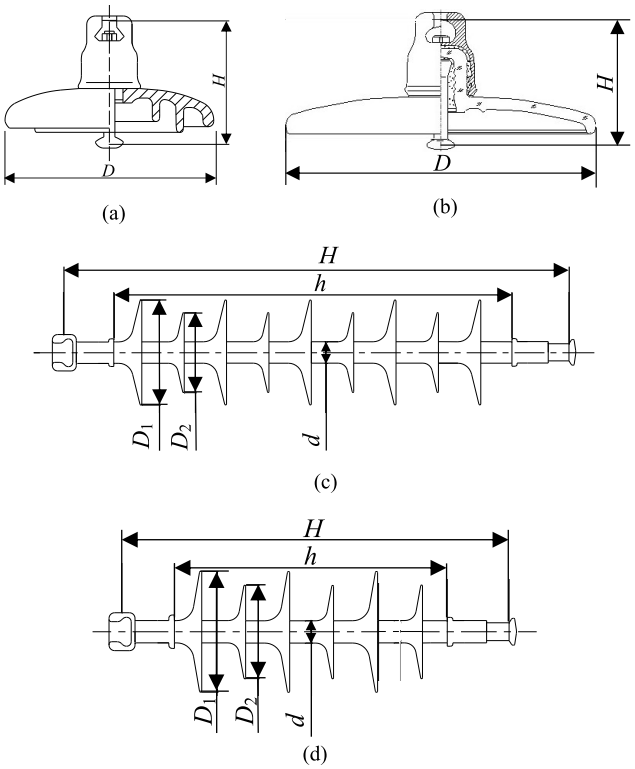

FIGURE 4. Profiles of the samples: (a) type A; (b) type B; (c) type C; (d) type d.

TABLE 1. Structural parameters of the samples.

Type	Materials	H	D	L
A	glass	147	261	320
B	glass	127	380	365
C	SIR	615	110/80	1375
D	SIR	320	125/90	540

B. TEST SAMPLES

The samples were four types of the insulators with two different surface materials, which were denominated by glass A, glass B, SIR C and SIR D, respectively. The structural parameters and profiles of the samples are shown in Figure 4 and Table 1, in which H is the structural height, D is the diameter of shed, and L is the creepage distance.

C. TEST PROCEDURES

1) PRETREATMENT OF SAMPLES

In the laboratory, the dirt and grease on the surface of the insulators was cleaned with deionized water, whose conductivity is less than 10 μS/cm.

Limited by conditions on site, deionized water is not available, so the pollutants on the insulators were removed with the groundwater, whose conductivity is less than 20 μS/cm.

For silicone rubber insulators, de-hydrophobic pretreatment was necessary to facilitate their polluting.

2) SAMPLES CONTAMINATION

The solid-layer method was utilized to pollute the insulator surfaces before snow accumulating in the chamber. Conductive and non-conductive materials were simulated with NaCl and Kaolin, respectively. Three different ESDDs were simulated, namely 0.05, 0.10 and 0.15 mg/cm. The ratio of ESDD to non-soluble deposit density was 1:4. The quality of two materials was determined by an electronic analytical balance. Then they were dissolved into deionized water and stirred evenly. The contaminated liquid was coated on the insulator surface with a brush manually.

To facilitate the tests, the dipping method in the field was adopted for contaminating the insulators to obtain the same polluting level as that in the chamber.

3) METHOD FOR SNOW ACCRETION ON THE INSULATORS

The relevant test standards for snow accumulation on the insulators are lack. The improved method that developed from the method proposed by Yaji *et al*. [22] was adopted. In [22], the artificial snow was generated, and then coated on the surface of the insulators by spraying manually. However, snowmaking and its accretion were conducted simultaneously in this study. The detailed test procedures are as follows [23], [24]. First, the insulators were suspended at a predetermined position in the chamber and water conductivity was adjusted to approximate 80 μS/cm. Second, the cooling system was turned on to stabilize the temperature at –9 – –13 °C. Then the sprinkling and speed regulation systems were turned on. The wind speed was controlled at about 3 m/s. The diameter of sprayed water droplets was in the range of 10 to 20 μm and then coated on the insulators in the form of snowflakes. Third, when snow accretion on the insulator met the requirements, the cooling, sprinkling and speed regulation systems were turned off.

In the field, before the snowfall was approaching, the pretreated insulators were hung on the test stand, and natural snowfall accreted on the insulator surface. If natural snowfall accumulation did not reach the required thickness, a manual coating was used to meet the test requirements.

4) FLASHOVER TESTS OF SNOW ACCRETED INSULATORS

After snow accretion on the insulators was completed, AC voltage was applied to obtain the minimum flashover voltage of snow-covered insulators by using the U-type method [25].

III. COMPARISON OF ELECTRICAL PERFORMANCE OF SNOW-ACCRETED INSULATORS IN THE CHAMBER AND IN THE FIELD

A. VISUAL OBSERVATION OF SNOW ACCRETION ON THE INSULATORS IN THE CHAMBER AND ON SITE

Figure 5 shows the appearances of snow-covered insulators in an artificial climate chamber and on site.

In Figure 5, the amount of the snowpack on the windward side of the insulators is greater than that on the leeward

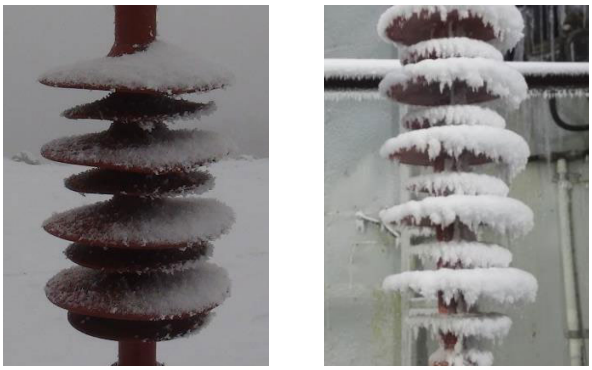

(a) (b)

FIGURE 5. Appearances of snow-covered insulators: (a) insulator in the field; (b) insulator in the chamber.

side under two different environments. The reasons can be explained by the following. Natural icing test base is a mountain pass type with a fixed wind direction in the winter. And the wind direction in the chamber is also fixed. Once the viscous fluid encounters obstacle like the insulator, its velocity is attenuated rapidly because of the blocking effect, and a boundary layer forms on the insulator surface. While the airflow blows towards the windward side of the insulator, its velocity is stratified. And the velocity within the boundary layer is much smaller than the inflow speed (Figure 6(a)). Therefore, in an environment convenient for snow accretion, when the snow particles move to the vicinity of the insulator with the airflow, their velocity decreases significantly because of the viscous effect of the airflow. The particles separated from the airflow collide with the windward side of the insulator and accumulate to form snowing. Meanwhile, the air flow through the leeward side flows backwards and a reflux vortex is observed because of the influence of backpressure gradient and fluid viscosity stagnation (Figure 6(a)). Affected by the backflow vortex, the particles accrete on the leeward side. From the particle trajectories shown in Figure 6(b), it is concluded that almost all the particles terminate in the rod and the shed facing the direction of the inflow. However, on the two sides that deviate from the direction of the incoming flow, the particles easily bypass the insulator with the air flow, which is not conductive to snow accreting. Therefore, the snow accumulation on the insulators is non-uniform.

B. INFLUENCE OF THE ESDD ON THE ELECTICAL PERFORMANCE OF SNOW-COVERED INSULATORS

Snow accretion on the insulator can be considered as a special type of icing. Hence, the flashover voltage of snow-covered insulators as a function of the ESDD can be depicted by the following equation [13]:

$$U_f = A \times \mathrm{ESDD}^{-n} \tag{1}$$

where U_f is the minimum flashover voltage of snow-covered insulator. A is a constant coefficient related to the material

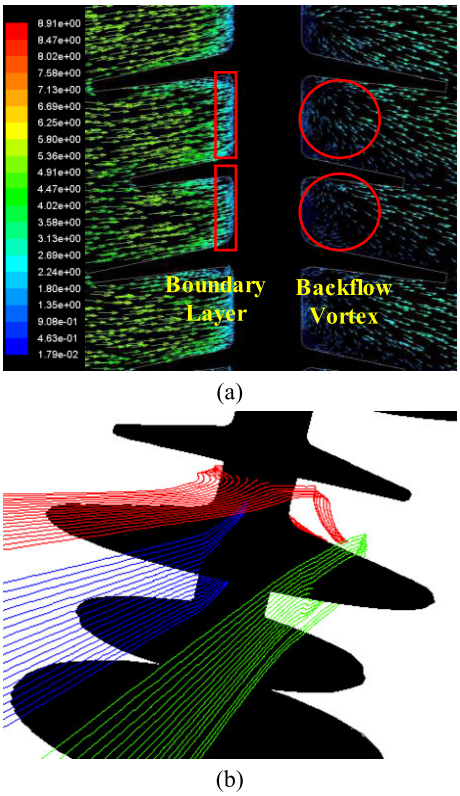

(a)

(b)

FIGURE 6. Gas-solid two-phase flow around the insulator: (a) distribution of the airflow field; (b) trajectories of the particles.

and structure of the insulator. n is an exponent describing the influent degree of the ESDD on U_f.

The results obtained in the chamber and on site cannot be compared directly because of the difference in altitude. The flashover voltage obtained in the field are corrected to that corresponding to an altitude of the chamber [26]:

$$\frac{P_N}{P_A} = \left(\frac{1 - H_N/45.1}{1 - H_A/45.1}\right)^{5.36} \tag{2}$$

$$U_C = \frac{U_f}{\left(P_N/P_A\right)^{n_0}} \tag{3}$$

where P_N and P_A are the pressure of the test base with an altitude of H_N and the pressure of the chamber with an altitude of H_A, respectively. U_C is corrected voltage. n_0 is the influence coefficient of air pressure on U_f. The preceding studies indicate that the values of n_0 for glass and silicone rubber insulators are approximate 0.5 [25]. Therefore, n_0 is taken as 0.5 in this paper.

To compare the flashover characteristics of the insulators with different structural configurations and leakage distances, an average arc flashover gradient is introduced to describe the electrical performance of snow-accreted insulators:

$$E_L = U_C/L = a \times ESDD^{-n} \tag{4}$$

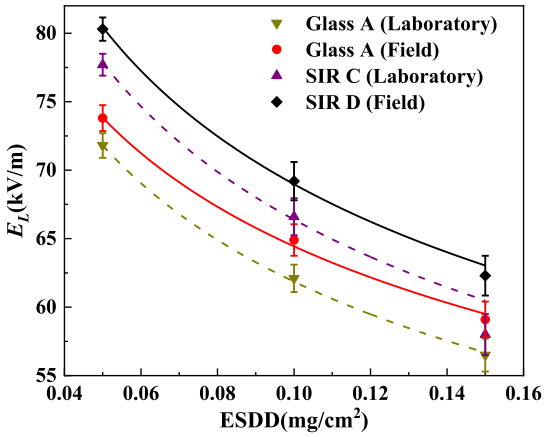

FIGURE 7. Variation of arc flashover gradient of snow-accreted insulators with ESDD.

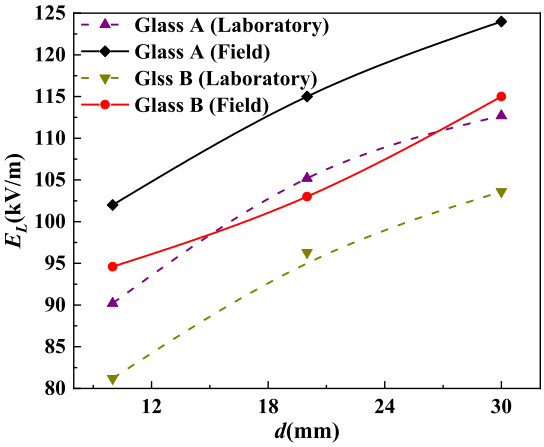

FIGURE 8. Variation of arc flashover gradient of snow-accreted insulators with d.

TABLE 2. Fitted values of a, n and R^2 according to equation (4).

Environment	Insulator	a	n	R^2
Laboratory	Glass A	37.7	0.215	0.999
	SIR A	39.1	0.230	0.991
Field	Glass A	41.0	0.196	0.988
	SIR B	41.4	0.222	0.997

where E_L is the average arc flashover gradient. L is the leakage distance of the insulator.

$$a = \frac{A}{\left(P_N / P_A\right)^{n_0}} \Big/ L \tag{5}$$

The flashover tests of snow-covered insulators were investigated to analyze the differences of the flashover characteristics in different environmental conditions. The results were fitted according to equation (4), as shown in Figure 7, where the thickness is 10 mm and ESDD is 0.05, 0.10 and 0.15 mg/cm^2. The fitted values of a, n and R^2 are listed in Table 2, in which R^2 is the determining coefficient indicating the correlation between the data and the formula.

The following conclusions can be drawn from Figure 7 and Table 2.

(1) The data has a high degree of fitting, and the error bar is within 8%. Therefore, the relationship between the AC arc flashover gradient and the equivalent salt deposit density is a power function with a negative exponent under two test environments.

(2) For the tested insulators, the E_L obtained in the field is higher than that determined from the chamber under the same pollution level. Taking silicone rubber insulator for instance, when the ESDD is 0.10 mg/cm^2, the arc gradients are 69.2 kV/cm and 66.6 kV/cm under the two test environments, respectively. The former is 3.90% higher than the latter. And the gap reaches 4.51% for a glass insulator.

C. INFLUENCE OF SNOW THICKNESS ON THE ELECTICAL PERFORMANCE OF SNOW-COVERED INSULATORS

Figure 8 shows the arc flashover gradient of snow-accreted insulators in an artificial climate chamber and on site, where snow thicknesses are 10, 20 and 30 mm, respectively, and the ESDD is 0.02 mg/cm^2. The water conductivity applied for snowing is 80 μS/cm in the chamber and this is less than 20 μS/cm in the field.

(1) In the range of our study, the arc flashover gradient increases with the increase of snow thickness whether under natural conditions or under the laboratory environment.

(2) There are two reasons for this. On one hand, the pollution on the insulator surface is dissolved into the water melted from snow to form a conductive water film, thereby reducing the residual resistance. However, the snow layer has a thermal insulation effect. Therefore, the thicker the snow layer on the insulator is, the harder it will melt. On the other hand, the snow layer is a porous medium with a capillary effect. The melted water may be partially absorbed by the snow layer. A thicker snow layer corresponds to absorbing more melted water. In this way, the power supply is required to provide more energy to make the melted water pass through the snow layer, thereby dissolving the pollution on the surface of the insulator. Therefore, the flashover voltage of snow accreted insulators is high for a thicker snowpack.

(3) However, the variation of flashover gradient with snow thickness is inconsistent with the results of silicone rubber insulators in [13], which is explained as follows. The distance between the adjacent sheds of silicon rubber insulator is much smaller than that of glass insulator. Snow accretion significantly changes its structure, resulting in the leakage distance not being effectively utilized, thereby reducing the flashover voltage.

(4) For the two types of tested insulators, the arc flashover gradient of artificial snow accretion is lower than that of natural snowfall at the same thickness. Taking glass B insulator for instance, when the thickness is 20 mm, the E_L of

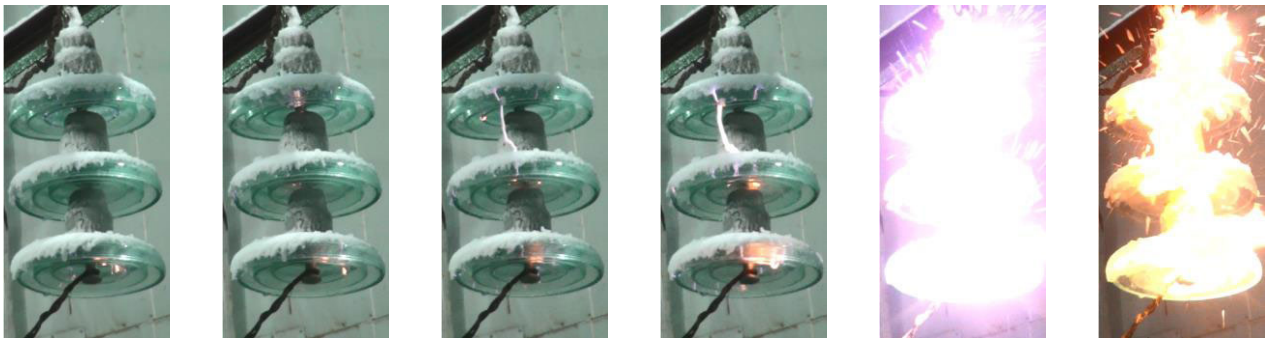

FIGURE 9. Sequence images of the flashover process of snow-covered glass A insulator in an artificial climate chamber.

natural snowfall is 103 kV/cm, and this value for artificial snow accretion is 96.3 kV/cm, which decreases by 6.50%. When the thickness is 30 mm, the values of E_L under two test environments are 115 and 103.6 kV/cm, respectively, and the former is 9.91% higher than the latter.

IV. ARC PROPAGATION ALONG THE SNOW-COVERED INSULATORS

A. FLASHOVER PROCESS OF AN INSULATOR COVERED WITH THE ARTIFICIAL SNOW IN THE CHAMBER

The discharge along the surface of the snow-covered insulator is a complex thermodynamic process related to snow melting, gas ionization, and generation and development of the local arc. To study the discharge mechanism in depth, the flashover process of snow-covered glass A insulator was recorded by a high speed camera in an artificial climate chamber, as shown in Figure 9, where the ESDD is 0.05 mg/cm^2 and snow thickness is 10 mm.

From Figure 9, the following conclusions can be concluded.

(1) As the applied voltage increased, the discharges first occurred at high-voltage end due to a relatively high current density (Figure 9(a)). Subsequently, the obvious discharges appeared on the lower surface of each insulator (Figure 9(b)). Moreover, their position was random.

(2) The discharges on the lower surface of the sheds mainly propagated along the leakage distance of the insulator with the increasing applied voltage, and gradually transformed into a white arc with a small diameter bridging the gap between adjacent sheds (Figure 9(c)). Furthermore, as the density of arc current increased, the diameter of the white arc became larger and its brightness was brighter (Figure 9(d)).

(3) At the moment of the flashover, the arc temperature was as high as 5000–6000 °C [27]. Thus, the air gap inside snow layer expanded sharply, causing snowpack to fall off the insulator in an explosive manner, as shown in Figure 9(e)–(f).

B. FLASHOVER PROCESS OF THE INSULATORS COVERED WITH NATURAL SNOWFALL IN THE FIELD

For comparison, the flashover tests were performed on the silicon rubber and glass insulators covered with natural snowfall at Xuefeng Mountain Natural Icing Test Base and the flashover processes are shown in Figure 10 and Figure 11, where the thickness is 10 mm and the ESDD is 0.05 mg/cm^2.

From Figure 10 and Figure 11, the conclusions can be summarized as follows.

(1) Compared with the discharges in Figure 9, the arc diameter during the flashover of snow-covered insulators in the field is larger with the following explanation. The decrease in air pressure reduces air density at high altitude, resulting in poor thermal conductivity of the air. When the accumulated heat is sufficient to induce thermal ionization, then the air around the arc changes from an insulated state to a conductive state, thereby increasing the cross-sectional area of the arc.

(2) According to the observation of the discharge phenomena during the flashover on site, the development of the local arcs does not propagate along the insulator surface, but deviate from the surface to form a arc levitation phenomenon. Taking glass A as an example, the distinct yellow arcs occurred on each insulator with the increasing applied voltage and they were tightly attached to the insulator (Figure 10(b)). These arcs consisted of two parts. One was on the upper surface of the insulator and the other was on the lower surface. As extending, all arcs on the upper surface float away from the insulator, while others on the lower surface still clung to the insulator (Figure 10(c)). Once the arc floating formed, the obvious discharge traces were observed at the arc channel. When the arcs on the second and third insulators developed to contact each other, the arc on the lower surface of the second insulator disappeared instantly, thereby forming a single arc discharge channel (Figure 10(d)–(e)). As the applied voltage continued to rise, the newly formed arc and the arc on the first insulator elongated, and then the two arcs were connected to form a complete arc (Figure 10(f)). Except that the arc on the lower surface of the third insulator was close to the surface, the rest floated in the air. An arc levitation was also observed in the flashover process of the silicon rubber insulator. However, there is no arc floating during the discharge of snow-covered insulators in the chamber.

(3) The arc levitation phenomenon can be explained as follows. The arcs on the insulator surface are mainly affected by electrostatic force, electromagnetic force and thermal

FIGURE 10. Sequence images of the flashover process of snow-covered glass A insulator at Xuefeng Mountain Natural Icing Test Base.

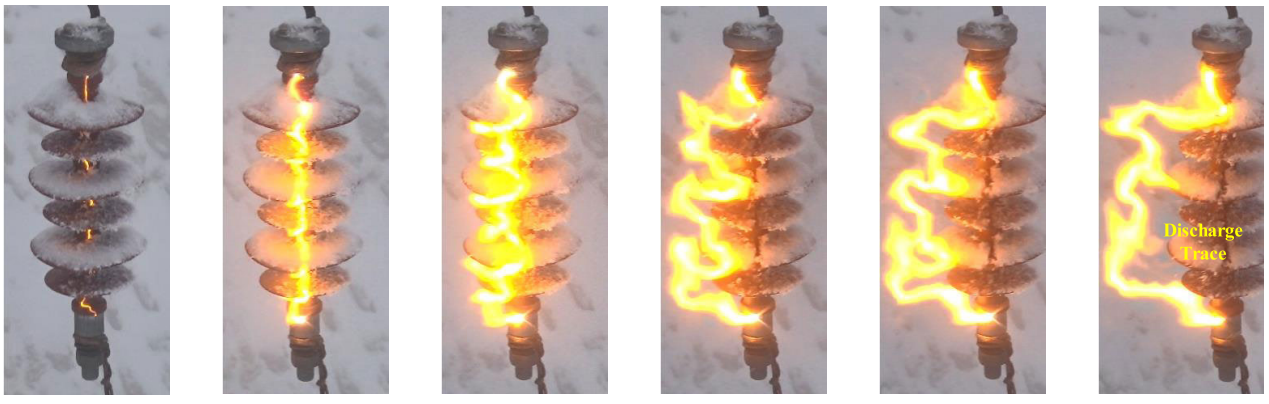

FIGURE 11. Sequence images of the flashover process of snow-covered SIR D insulator at Xuefeng Mountain Natural Icing Test Base.

buoyancy during the development of discharges [28]:

$$\begin{cases} F_e = \varepsilon_0 E^2 r_a^2 / 2 \\ F_m = \mu_0 r_a^2 \left[I / (2\pi r_a) \right]^2 / 2 \\ F_t = \rho g \left(\pi r_a^2 \right) r_a \end{cases} \tag{6}$$

where F_e, F_m and F_t represent electrostatic force, electromagnetic force and thermal buoyancy, respectively. ε_0 is the permittivity of vacuum. E is the electric field strength of the arc root. r_a is the arc radius. μ_0 is the permeability of vacuum. I is the arc current. ρ is the air density. g is the gravitational acceleration.

The results showed that for a snow-covered insulator, the relationship between the arc current and its radius can be expressed as [20]:

$$r_0 = \sqrt{\frac{I}{2.439\pi}} \tag{7}$$

where r_0 is the arc radius.

The arc radius increases with the decreasing air pressure, which can be expressed as follows [29]:

$$r_a = \sqrt{\frac{I}{2.439\pi}} \left(\frac{P}{P_0} \right)^{-0.465} \tag{8}$$

where P is the pressure at high altitude and P_0 is the standard atmospheric pressure.

Considering the influence of the pressure on the electric field, the relationship between the arc gradient and the current can be approximated by the following equation [21], [25]:

$$E = 100.25 \times \left(\frac{P}{P_0} \right)^{0.5} \times I^{-0.66} \tag{9}$$

The pressure as a function of the altitude can be depicted by the following [25]:

$$\frac{P}{P_0} = \left(1 - \frac{H}{45.1} \right)^{5.36} \tag{10}$$

Substituting equations (7)–(10) into equation (6) yields the following formulas:

$$\begin{cases} F_e = 5.807 \times \left(P/P_0 \right)^{0.07} \times I^{-0.32} \times 10^{-9} \\ F_m = 1.592 \times I^2 \times 10^{-8} \\ F_t = 1.880 \times \dfrac{293}{273 + t} \times \left(P/P_0 \right)^{-0.395} \times I^{1.5} \times 10^{-6} \end{cases} \tag{11}$$

The temperature of the partial arc during the discharge development is generally 5000–6000 °C, resulting in a

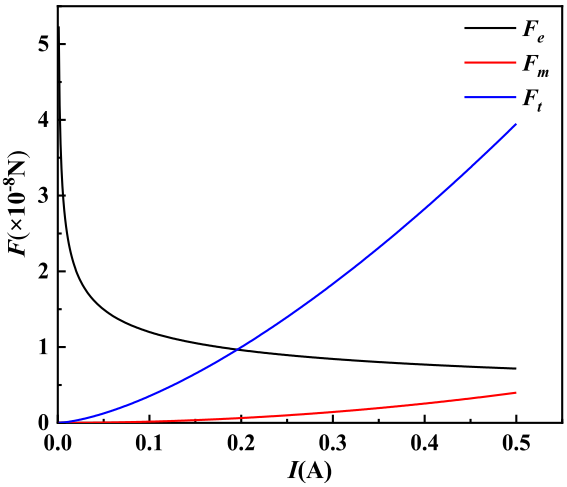

FIGURE 12. The relationship between the forces applied to the arc and arc current.

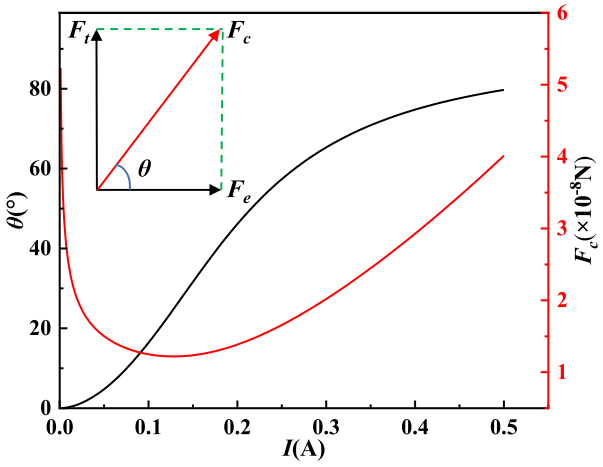

FIGURE 13. The relationship between the magnitude and direction of the comprehensive forces applied to the arc and arc current.

sharply increase in the temperature of the surrounding air. From equation (11), the thermal buoyancy decreases as the temperature increases. Assuming that the air temperature around the arc is basically the same as that of the arc, the arc is considered to be 5000 °C [27], and the forces are calculated by equation (11), as shown in Figure 12.

In Figure 12, when the arc current is less than 0.2 A, the electrostatic force dominates. Otherwise, the thermal buoyancy is predominant. Compared with electrostatic force and thermal buoyancy, the electromagnetic force applied to the arc is relatively small, hence, it can be ignored. Therefore, the combined force of electrostatic force (F_e) and thermal buoyancy (F_t) is defined as comprehensive (F_c) and the angle between F_e and F_c is defined as θ.

The magnitude and direction of F_c during the development of the partial arc varies with the current, as shown in Figure 13.

When the obvious local arcs just form, the electrostatic force plays a leading role. Since its direction is approximately

FIGURE 14. Observation of snow-covered insulators: (a) insulator in the field; (b) insulator in the chamber.

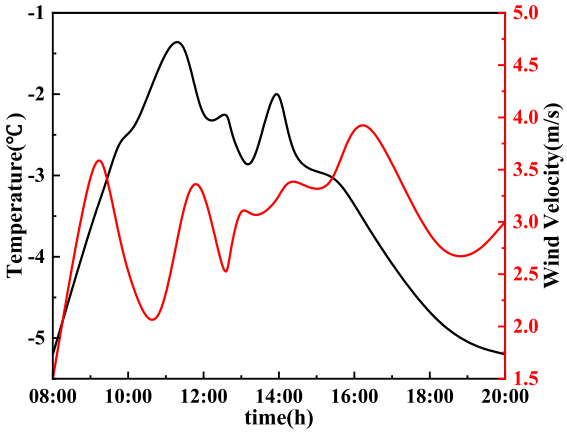

FIGURE 15. Variation of air temperature and wind speed with time in a day at Xuefeng Mountain Natural Icing Test Base.

paralleled to the surface of the insulator, the partial arc extends and develops along the insulator. As the applied voltage increases, the arc current increases. The thermal buoyancy dominates, and its direction is approximately perpendicular to the insulator, which causes the local arcs on the lower surface to cling to the insulator, however, the arcs on the upper surface float away from the insulator, forming an obvious arc floating phenomenon.

V. DISCUSSION AND ANALYSIS

In this paper, the insulator covered with natural snowfall was performed at Xuefeng Mountain Natural Icing Test Base with an altitude of 1400 m. The altitude of artificial climate chamber is 232 m. Because of the low air pressure and low air density at high altitudes, the local arc dissipates less heat due to air convection. In addition, from Section IV the arc levitation is observed during the flashover of snow-accreted insulators in the field, thereby causing the creepage distance not being effectively utilized. As a result, the flashover voltage of snow-covered insulator at high altitudes should be lower than that in the chamber. However, the results are reversed for the following explanation.

A. DIFFERENCES IN ENVIRONMENTAL PARAMETERS DURING THE SNOW ACCRETION TESTS

Environmental parameters, including temperature, humidity and wind speed, *et al.*, are controllable constants in the artificial climate chamber. However, they are uncontrollable in

the natural environment and fluctuate within a small range in a short period of time, resulting in differences in the distribution, density and compactness of the snowpack between natural test and artificial simulation, as shown in Figure 14.

B. DIFFERENCES IN ENVIRONMENTAL PARAMETERS DURING THE FLASHOVER TESTS

The ambient temperature is constant and the wind speed is 0 in the flashover process of the insulators covered with the artificial snow. However, the temperature fluctuates and the wind speed varies in the field, as shown in Figure 15. The electrons generated by the discharges accelerate to diffuse under the action of wind, which affects the extension and development of the arcs on the surface of the insulators.

VI. CONCLUSION

1. When viscous fluid encounters obstacles, a boundary layer forms. Its internal velocity is very low, which is conductive to snow accumulation on the insulators. Due to the fixed wind direction, the amount of snow accretion on the windward side is greater than that on the leeward side under natural and artificial simulation environments.

2. For the tested insulators, the arc flashover gradient of snow-covered insulators in the chamber is lower than that in the field. Furthermore, the flashover gradient decreases in a power function with the increasing equivalent salt deposit density. However, for a glass insulator, the flashover gradient increases with the increasing snow thickness because of the adiabatic effect and capillary action.

3. When the arc current is less than 0.2 A, the electrostatic force in the direction parallel to the insulator dominates, causing the arc attaching to the insulator surface tightly. With the increase of the current, the thermal buoyancy in the direction perpendicular to the insulator plays a major role, and then the arc floating forms. Compared with the above two forces, the electromagnetic force is so small that it can be ignored in the study of the discharge development of snow-covered insulators.

4. Due to the difference of environmental parameters between the climate chamber and the site, the distribution, interlaminar alternation and compactness of artificial snow accumulation on the insulator are not equivalent to those of natural snowfall accretion, which results in the difference of the electrical performance of snow-covered insulators under the two test environments. Therefore, more attention should be paid to studying their equivalence to provide the best design reference for the external insulation of transmission lines in snowy regions.

REFERENCES

[1] L. Yang, X. Jiang, Y. Hao, L. Li, H. Li, R. Li, and B. Luo, "Recognition of natural ice types on in-service glass insulators based on texture feature descriptor," *IEEE Trans. Dielectr. Electr. Insul.*, vol. 24, no. 1, pp. 535–542, Feb. 2017.

[2] J. Lu, B. Wang, Z. Fang, Z. Jiang, J. Hu, and W. Wu, "Study on the flashover performance of an anti-thunder composite insulator under ice accretion conditions for a 10 kV distribution line," *IEEJ Trans. Electr. Electron. Eng.*, vol. 13, no. 12, pp. 1738–1746, Dec. 2018.

[3] M. M. Hussain, M. A. Chaudhary, and A. Razaq, "Mechanism of saline deposition and surface flashover on high-voltage insulators near shoreline: Mathematical models and experimental validations," *Energies*, vol. 12, no. 19, p. 3685, Sep. 2019.

[4] Y. Huang, X. Jiang, and M. S. Virk, "Study of inverted T-shape insulator strings in icing conditions," *Cold Regions Sci. Technol.*, vol. 173, May 2020, Art. no. 103021.

[5] Y. Hu, X. Jiang, L. Xie, Z. Zhang, Q. Wang, and Y. Pan, "Influence of electric field strength on crystallization effect during phase transition," *High Voltage Eng.*, vol. 44, no. 6, pp. 2074–2080, Jun. 2018.

[6] X. Jiang, Z. Zhang, Q. Hu, J. Hu, and L. Shu, "Thinkings on the restrike of ice and snow disaster to the power grid," *High Voltage Eng.*, vol. 44, no. 2, pp. 463–469, Feb. 2018.

[7] Y. Liu, L. Shu, X. Jiang, Q. Hu, H. Yang, Z. Yu, and M. Zhu, "Study on conductive ions distribution in icicles of ice-covered insulators," *Int. J. Electr. Power Energy Syst.*, vol. 116, Mar. 2020, Art. no. 105567.

[8] X. Jiang, M. Zhu, L. Dong, Q. Hu, Z. Zhang, and J. Hu, "Site experimental study on suspension-tension arrangement for preventing transmission lines from icing tripping," *Int. J. Electr. Power Energy Syst.*, vol. 119, Jul. 2020, Art. no. 105935.

[9] X. Jiang, Q. Hu, Q. Wang, J. Hu, Z. Zhang, L. Shu, and Y. Hu, "Crystallisation effect of conductive ions in freezing water during phase transition and its effect on ice flashover voltage," *IET Gener., Transmiss. Distrib.*, vol. 10, no. 9, pp. 2147–2154, Jun. 2016.

[10] M. M. Hussain, S. Farokhi, S. G. Mcmeekin, and M. Farzaneh, "Mechanism of saline deposition and surface flashover on outdoor insulators near coastal areas part II: Impact of various environment stresses," *IEEE Trans. Dielectr. Electr. Insul.*, vol. 24, no. 2, pp. 1068–1076, Apr. 2017.

[11] A. Takei, T. Mizuma, M. Akatsuka, and T. Yamada, "Large-scale numerical electrostatic analysis for performance evaluation of insulators with accreted icicles," *Int. J. Appl. Electromagn. Mech.*, vol. 60, no. 2, pp. 187–207, May 2019.

[12] M. M. Hussain, S. Farokhi, S. G. Mcmeekin, and M. Farzaneh, "Prediction of surface degradation of composite insulators using PD measurement in cold fog," in *Proc. IEEE Int. Conf. Dielectr. (ICD)*, Montpellier, France, Jul. 2016, pp. 697–700.

[13] Y. Hu, S. Guo, R. Xian, X. Han, Z. Yang, and Y. Wu, "Flashover performance and process of suspension insulator strings artificially covered with snow," *Energies*, vol. 11, no. 11, p. 2916, Oct. 2018.

[14] X. Jiang, S. Guo, J. Hu, Y. Hu, and H. Yang, "Influence of snow accretion with different shape on negative DC flashover characteristics of suspension insulators," *Trans. China Electrotech. Soc.*, vol. 33, no. 2, pp. 451–458, Jan. 2018.

[15] M. M. Hussain, S. Farokhi, S. G. Mcmeekin, and M. Farzaneh, "Effect of uneven wetting on E-field distribution along composite insulators," in *Proc. IEEE Electr. Insul. Conf. (EIC)*, Montreal, QC, Canada, Jun. 2016, pp. 69–72.

[16] K. Yaji and H. Homma, "Insulator flashover caused by salt- contaminated snowstorms–lessons from the snow damage in japan," *IEEE Elect. Insul. Mag.*, vol. 35, no. 1, pp. 23–37, Jan. 2019.

[17] R. Zhang, J. Li, M. Wang, C. Zhang, M. Lu, and Z. Liu, "Flashover characteristics of snow-covered post insulators in substations," *High Voltage Eng.*, vol. 42, no. 12, pp. 3823–3829, Dec. 2016.

[18] Y. Li, Y. Teng, S. Yuan, and O. Leng, "Study on snow covered insulator flashover characteristics and its improved QNN prediction model," *Power Syst. Tech.*, vol. 42, no. 8, pp. 2725–2731, Aug. 2018.

[19] H. Homma, K. Yaji, T. Aso, M. Watanabe, G. Sakata, A. Dernfalk, and I. Gutman, "Evaluation of flashover voltage property of snow accreted insulators for overhead transmission lines, part III–154 kv full-scale flashover voltage test of snow accreted insulators -," *IEEE Trans. Dielectr. Electr. Insul.*, vol. 21, no. 6, pp. 2568–2575, Dec. 2014.

[20] H. Hemmatjou, M. Farzaneh, and I. Fofana, "Modeling of the AC arc discharge on snow-covered insulators," *IEEE Trans. Dielectr. Electr. Insul.*, vol. 14, no. 6, pp. 1390–1400, Dec. 2007.

[21] Z. Zhang, X. Qiao, Y. Zhang, L. Tian, D. Zhang, and X. Jiang, "AC flashover performance of different shed configurations of composite insulators under fan-shaped non-uniform pollution," *High Voltage Eng.*, vol. 3, no. 3, pp. 199–206, Sep. 2018.

[22] K. Yaji, H. Homma, G. Sakata, and M. Watanabe, "Evaluation on flashover voltage property of snow accreted insulators for overhead transmission lines, part I—Field observations and laboratory tests to evaluate snow accretion properties," *IEEE Trans. Dielectr. Electr. Insul.*, vol. 21, no. 6, pp. 2549–2558, Dec. 2014.

[23] M. M. Hussain, S. Farokhi, S. G. McMeekin, and M. Farzaneh, "Effect of cold fog on leakage current characteristics of polluted insulators," in *Proc. Int. Conf. Condition Assessment Tech. Elect. Syst.*, Bengaluru, India, Apr. 2016, pp. 163–167.

[24] M. M. Hussain, S. Farokhi, S. G. Mcmeekin, and M. Farzaneh, "Impact of wind on pollution accumulation rate on outdoor insulators near shoreline," in *Proc. IEEE Int. Power Modulator High Voltage Conf. (IPMHVC)*, San Francisco, CA, USA, Jul. 2016, pp. 453–456.

[25] X. Jiang, L. Shu, and C. Sun, "Test method for iced insulators," in *Insulation of Electric Power System Under Pollution and Icing Conditions*. Beijing, China: China Electric Power Press, 2009.

[26] Z. Zhang, Y. Cheng, J. Zhao, X. Jiang, and C. Fan, "AC flashover performances of artificial icing and nature icing for XP-160 insulator string," *High Voltage Eng.*, vol. 44, no. 9, pp. 2777–2784, Sep. 2018.

[27] A. Nekahi and M. Farzaneh, "Rotational temperature measurement of an arc formed over an ice surface," *IEEE Trans. Dielectr. Electr. Insul.*, vol. 18, no. 3, pp. 755–759, Jun. 2011.

[28] W. Sima, W. Tan, Q. Yang, B. Luo, and L. Li, "Long AC arc movement model for parallel gap lightning protection device with consideration of thermal buoyancy and magnetic force," *Proc. CSEE*, vol. 31, no. 19, pp. 138–145, Jul. 2011.

[29] M. Farzaneh, J. Zhang, and Y. Li, "Effects of low air pressure on AC and DC arc propagation on ice surface," *IEEE Trans. Dielectr. Electr. Insul.*, vol. 12, no. 1, pp. 60–71, Feb. 2005.

YUYAO HU was born in Heze, Shandong, China, in 1989. He received the B.S. degree in electrical engineering from the Inner Mongolia University of Science and Technology, Inner Mongolia, in 2012, and the Ph.D. degree in electrical engineering from Chongqing University, Chongqing, in 2017. He is currently a Lecturer with the College of Electrical and Electronic Engineering, Shandong University of Technology. His current research interest includes the selection of external insulation for transmission.

XINGLIANG JIANG (Senior Member, IEEE) was born in Hunan, China, in 31 July 1961. He received the M.Sc. and Ph.D. degrees from Chongqing University, Chongqing, China, in 1988 and 1997, respectively. His employment experiences include the Shaoyang Glass Plant, Shaoyang, Hunan; the Wuhan High Voltage Research Institute, Wuhan, Hubei; and the College of Electrical Engineering, Chongqing University. He has published his first monograph-Transmission Line's Icing and Protection, in 2001, and has published over 120 articles about his professional work. His research interests include high-voltage external insulation and transmission line's icing and protection. He received the First-Class Reward of National Technology Improvements, in 2013, the Second-Class Reward for Science and Technology Advancement from the Ministry of Power, in 1995, Beijing Government, in 1998, and the Ministry of Education, in 1991 and 2001, the First-Class Reward for Science and Technology Advancement from Ministry of Power, in 2004, the Third-Class Reward for Science and Technology Advancement from the Ministry of Power, in 2005, the Second-Class Reward for Science and Technology Advancement from the Ministry of Technology, in 2005, the First Class Reward for Science and Technology Advancement from the Ministry of Education, in 2007, and the First-class Reward for Science and Technology Advancement from Chongqing City, in 2007.

SIHUA GUO was born in Shaoyang, Hunan, China, in 1992. She received the B.S. degree in electrical engineering from the South China University of Technology, Guangdong, in 2014, and the M.Sc. degree in electrical engineering from Chongqing University, Chongqing, in 2017. She is currently working with the State Grid Chongqing Electric Power Research Institute. Her main research interest includes high-voltage external of transmission lines.

ZHONGYI YANG was born in Chongqing, China, in 1990. He received the B.S. degree in electrical engineering from Chongqing University, Chongqing, in 2013, where he is currently pursuing the Ph.D. degree with the School of Electrical Engineering. His current research interest includes the study of anti-pollution measures for insulators.